

# How to present/report results in a research posters

Dr Ana Doblas

Dr. Claudio Meier

The University of Memphis

PD UofM Spain Program

Monday, July 17<sup>th</sup>, 2023

Driven by  
doing.



THE UNIVERSITY OF  
MEMPHIS®

# Objective of the session

At the end of the session, students will be able to

1. Learn the top points for preparing a good poster
2. Identify best software for drafting a poster
3. Understand general layout of a poster
4. Recognize good/bad posters in terms of colors, information and figures

# What is a Research Poster?

- **Research posters summarize information or research concisely and attractively to help publicize it and generate discussion**
- **A poster is usually a mixture of a brief text mixed with tables, graphs, pictures and other presentation formats**
- **At a conference, the presenter stands by the poster display while other participants can come and view the presentation and interact with the author.**



**Most conferences include poster presentation in their programs**

# Why do we present or discuss a poster?

- A poster session is a good opportunity to present yourself and your research in a favorable light, make contacts and get useful feedback

**Include your contact information**

- Competitions for audience's time → capture audience's attention and communicate your message quickly and succinctly.

**Tell why matters, what you did, what you found and what you recommend**

# Top Pointers for a Good Poster

1. Know your audience to communicate to them effectively
2. Text should be large enough to be seen from 5 feet away
3. Sections should be organized in a way that leads the viewer through the display. (Consistent and clean layout)
4. Make illustrations simple and bold.
5. Effective use of graphics
6. Display should be self-explanatory so you are free to talk

# Top Pointers for a Good Poster

## 6. Keep display simple and text brief

A viewer should “get it” in 30 seconds.

## 7. A neutral colored poster on matte board is more pleasing to the eye than one on a bright colored background

## 8. Organize your material and edit your content to eliminate distracting visual noise

## 9. Use of bullets, numbering, and headlines make it easy to read

# Top Pointers for a Good Poster

**10. Title is shows and should draw interest.**

**11. Word count of about 300 to 800 words.**

**12. Text is clear and to the point.**

**13. Include references, acknowledgments, authors' names and institutional affiliations**

**14. Revise the Guidelines for Presenters provided by the conference organization**

# Where do I begin?

Answer these three questions:

1. What is the most important/interesting finding from my research project?
2. How can I visually share my research with conference attendees? Should I use charts, graphs, photos, images?
3. What kind of information can I convey during my talk that will complement my poster?

**KEEP IT SIMPLE**



# What software can I use to make a poster?

**PowerPoint**: a popular, easy-to-use option.

**Adobe Illustrator, Photoshop and InDesign**: feature-rich professional software that is good for posters including lots of high-resolution images.

**Open Source Alternative**: OpenOffice is the free alternative of PowerPoint. Inkscape and Gimp are alternatives to Adobe products.

# General layout

**Template for dimensions dictated by the organization**

**Authors, Presenter name highlighted**

Authors' organization

**Introduction**

**Methods**

**Results**

**Conclusions**

**Aims**

**Background**

**References**

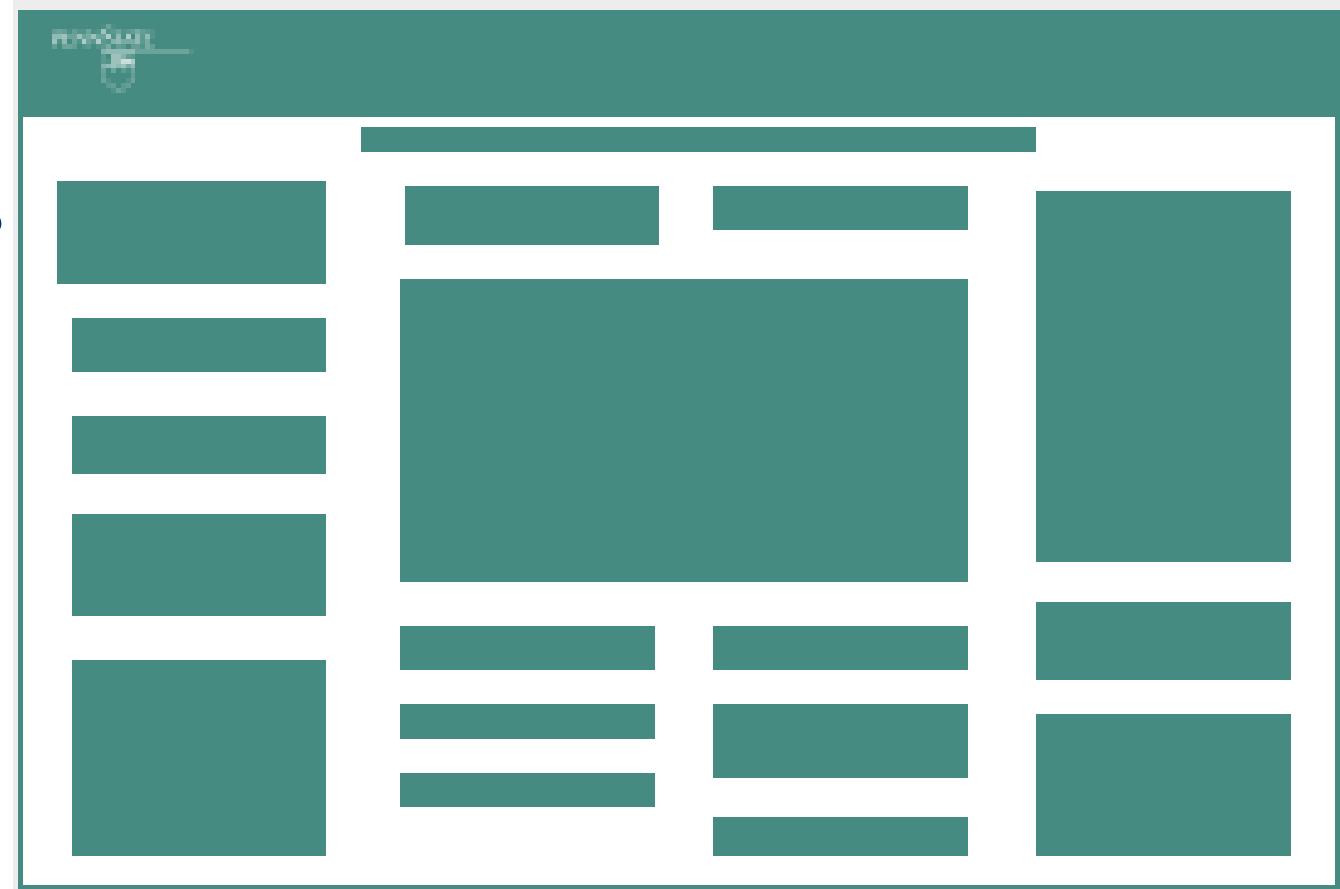
**Acknowledgement**

# How to make a neat layout

Try to keep 40% of the poster area empty of text and images

Limit the use of boxes and lines

If items go together, put them close to each other



# Selecting Fonts and Using Text

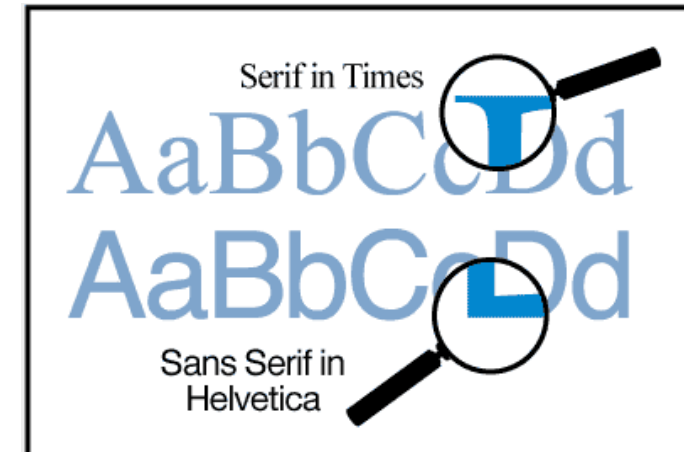
**Use Sans Serif fonts (*Helvetica, Arial*) for titles, headlines or labels**

**Use common Serif fonts (*Times Roman*) for body text**

**Do not use more than 3 fonts**

**Combine uppercase and lowercase letters**

**Text has to stand out clearly against the background**



# Choosing and Using Color

Are there any colors natural to your project? Blue for ocean studies

Maintain a color scheme

Keep backgrounds subtle.

Use bright and saturated colors sparingly

**CLAIMS**

Large amounts of red, yellow or orange can overpower your message



# Using Images

*Questions to ask: Do you have photos that were taken during your work? Did you create graphs and charts that could be simplified and colorized? Images to point out key points of your message?*

**Use meaningful, high-quality images**

**Adjust color and contrast in images**

**Crop and edit images so the important information is obvious**

**Add short titles or captions to the images**

**Always attribute borrowed images**

**Include labels. Avoid separate keys.**

# Where to place your images

Place your images so they are balanced visually in the poster and they help to the story's flow



## Remember

- Images should be spread evenly over the poster surface, pulling the viewers eyes to all areas.
- Lead the viewer through the material

# Attitude and body language

- **Show up early and set up the poster**
- **Dress appropriately**
- **Stay with your poster**
- **Ask if people want an explanation**
- **Use the poster for talking points**



# Other things to consider

- **Prepare 3-5 minutes of explanation**
- **Understand EVERYTHING you present**  
Scientifics can see right through you when you don't
- **Be deep in your knowledge**  
Show that you have the proper knowledge  
More specific question of the audience  
More deep discussion than a conference

# Videos to be watched

- **Making a better research poster by American Journal Experts**  
[https://www.youtube.com/watch?v=AwMFhyH7\\_5g](https://www.youtube.com/watch?v=AwMFhyH7_5g)
- **How to Present an Academic Research Poster**  
<https://www.youtube.com/watch?v=0ozwCEeaVWE>
- **How to make a scientific poster that people want to stop at by EMNL**  
<https://www.youtube.com/watch?v=PwJu7H66T3Y>

# We have promoted and fostered undergraduate research using a required technical communication course



**Jenny Lo**  
Engineering Education  
Virginia Tech

**Lisa McNair**  
Engineering Education  
Virginia Tech

**Whitney Edmister**  
Enhancement of Engineering Diversity  
Virginia Tech

**Michael Alley**  
College of Engineering  
Penn State



## Introduction

The Boyer Commission Report has urged universities to “make research-based learning the standard” for the education of undergraduates.

One idea to promote undergraduate research is to use an option in the traditional technical communication course, which many engineering curricula already require. This project assesses such an option in the College of Engineering at Virginia Tech.



Undergraduate Research Experiences  
Summer

## Research Experiences: Summers 2005 and 2006

Army Research Laboratory  
East Tennessee State University  
MIT  
Univ. of Illinois at Urbana-Champaign  
Univ. of South Carolina  
Vanderbilt University  
Woods Hole Oceanographic Institution

Bucknell  
Georgia Tech (2 students)  
Penn State (2 students)  
Univ. of Karlsruhe  
Univ. of Virginia  
Virginia Tech (17 students)

I can not see the structure



Preparing for Research (1-credit)  
Spring



Documenting Research (2-credits)  
Fall

## Results

Number of students: 05 course  
% of students: underrepresented groups  
% of enrollees who obtained offers for funded summer research positions  
Participants in 2005 research symposium (trigger for 06 course)  
Number of students: 06 course  
% of students: underrepresented groups  
% of enrollees who obtained offers for funded summer research positions  
Participants in 2006 research symposium (trigger for 07 course)

## Goal Outcome

25	20
40%	55%
100%	100%
25	42
25	16
40%	37.5%
100%	87.5%
25	21



## Conclusions

The tested course has been a success at promoting and fostering research among undergraduates, especially those from underrepresented groups.

Two students have won NSF Graduate Research Fellowships. In addition, several students have achieved professional publications from their summer research:

5 conference papers      Students as lead authors  
5 journal papers         Students as co-authors

The main problem has been the logistics of a 2-semester course sequence. Next year, at Penn State, we will attempt a 1-semester version that follows the summer research experience and that is preceded by preparation workshops in the spring.



Undergraduate Research Symposium  
Fall

# Same format for sections' and figures' titles

## Abstract

Identification of novel drug targets in ovarian cancers has focused on expression of genes in the tyrosine kinase family. We have previously shown that the spleen tyrosine kinase (SYK) gene was expressed in 73% of 55 ovarian cancer specimens, compared to 26% of 60 breast cancer specimens. Previous studies established the role of SYK in tumor progression. Among its many targets, SYK can bind microtubules and other molecules associated with the cytoskeleton. We found SYK to be expressed in 6 of 10 ovarian carcinoma cell lines. Because of the ability of SYK to bind to microtubules, we studied the relationship of SYK expression to cellular migration. We examined several ovarian cancer cell lines that variably express SYK to elucidate the potential effects of SYK on cell migration. Our results demonstrate that knockdown of SYK expression by siRNA resulted in a decreased capability of cells to migrate using a traditional wound scratch assay. The duration of this effect was dependent upon cell line used suggesting that additional protein targets may be involved in the migratory process. The potential effects of SYK expression on invasion are currently being investigated. We will evaluate potential upstream and downstream targets to elucidate the pathway(s) responsible for SYK effects and compare within the cell lines examined. Understanding the growth signals and proteins potentially responsible for invasion and metastasis in ovarian cancer cell lines and tumor samples may eventually lead to new therapeutic approaches for ovarian cancers.

## Background

Ovarian epithelial cancers are the leading cause of death from gynecological malignancies in the United States with 21,550 new cases and 14,600 deaths estimated for 2009 (1). The high mortality results from the fact that ~70% of these cases are diagnosed at a late stage (2), and that standard therapies using platinum-based drugs and taxanes have reached their ceiling of effectiveness (3-5).

With the goal of further understanding signaling pathways in this disease, we examined our ovarian cancer microarray data (6), and found that spleen tyrosine kinase (SYK) was overexpressed in a majority of the specimens.

Syk is a non-receptor type protein kinase that has a well-known role in lymphocyte development and activation of immune cells (7). It targets adaptor molecules, facilitates signaling associated with the inflammatory response, regulates binding of b2-integrins, and binds microtubules and molecules associated with the cytoskeleton (7). Physiologically, it appears to play a role in cellular adhesion, immune recognition, platelet activation, and vasculogenesis (8, 9).

The role of Syk in epithelial malignancies is not well understood. In breast (8, 11), gastric (12), pancreatic cancers (13) SYK expression is low, whereas it is highly expressed in some cases of nasopharyngeal (14), head and neck cancers (15), and anaplastic large cell lymphomas (9).

Because SYK was expressed in 75% of our ovarian cancer clinical specimens, in contrast to breast cancers, we chose to initially study the relevance of Syk in cellular proliferation and metastasis.



## SYK promotes tumor progression in ovarian cancer cell lines.

Aya Sultan<sup>1</sup>, Cindy Y. Wang<sup>2</sup>, George E. Duran<sup>2</sup>, E. Brian Francisco<sup>2</sup>, Jonathan S. Berek<sup>1</sup>, and Branimir I. Sikic<sup>2</sup>

Division of Gynecologic Oncology, Department of Obstetrics & Gynecology<sup>1</sup> and Division of Oncology, Department of Medicine<sup>2</sup>, Stanford University School of Medicine, Stanford, CA 94305-5151

Supported by NIH R01 CA 114037 from the U.S. Public Health Service (Sikic) and the Ovarian Cancer Research Fund (OCRF)

#1401

## Materials and Methods

**Cell Culture.** Ovar 3 cancer cell line was obtained from the American Type Culture Collection (ATCC, Manassas, VA).

**Drugs.** Paclitaxel was obtained from Sigma Aldrich (St. Louis, MO). Stock solutions were stored at -20°C. Syk-specific and Neg-siRNA were obtained from Invitrogen (St. Louis, MO). Stock solutions were stored at -20°C. Specific Syk inhibitors P505-1 (PRT06027) was supplied by Purto Pharmaceuticals, Inc. (South San Francisco, CA).

**Measurement of Cytotoxicity.** The cytotoxicity of various compounds was determined using a modified SRB colorimetric cell proliferation assay<sup>34</sup> after a 72 hr drug incubation.

**ELC Detection of Relevant Proteins.** Anti-syk and anti-actin (Santa Cruz Biotechnology, Inc., Santa Cruz, CA) were used as the primary antibodies, recognized by either rabbit anti-mouse or donkey anti-rabbit IgG-conjugated secondary antibodies (Santa Cruz Biotechnology, Inc.; Santa Cruz, CA), and detected by ECL reagents (Amersham Pharmacia Biotech; Piscataway, NJ).

**Silencing Experiments.** The Syk-specific siRNA and a non-targeting control (Ambion neg siRNA; Gaithersburg, VA) were introduced by Lipofectamine RNAiMax transfection.

**Annexin V and PI Staining for Apoptosis by Flow Cytometry.** Genescreen's Apoptosis Detection Kit (catalog L00286, Piscataway, NJ) was used to detect apoptotic cells following treatment with taxanes. Briefly, cells were treated with taxanes for the desired time, harvested using trypsin without EDTA, and stained with an enhanced green fluorescent protein (EGFP) fused with annexin V and propidium iodide (PI). Following a 15 min incubation at room temperature away from light, annexin V-EGFP binding was detected by flow cytometry using a FITC signal detector (FL1), and PI staining by phycoerythrin (PE) signal detector (FL2). 10,000 events/cell were collected at the Stanford Shared FACS Facility, and FACS plots were compared to an untreated control.

**Immunostaining.** Briefly, cells were blocked in Blocking Buffer, which was subsequently aspirated and the diluted primary antibody was applied and incubated overnight at 4°C. PRIS wash was performed then the cells were incubated in fluorochrome-conjugated secondary antibody for 1-2 hours at room temperature in dark. Another PRIS wash was then performed. Slides were then covered with coverslips with ProLong Gold Antifade Reagent and mounting medium with DAPI staining was added. Slides were kept in the dark and allowed to dry overnight. Slides were examined under a fluorescent microscope at 10x magnification. All incubations were carried out at room temperature unless otherwise noted in a humid light-tight box or covered dish to prevent drying and fluorescence fading.

## Summary

The SYK gene was expressed in 73% of our ovarian cancer clinical specimens, in contrast to breast cancers, which demonstrated minimal to absent expression in 73% of our breast clinical cancer specimens.

Differential Syk protein expression was observed in our ovarian cancer cell lines with 6 of the 10 lines expressing Syk.

The use of RNAi to silence SYK in OVCAR-3 cells resulted in decreased cell density and was dependent on kinase activity. This decrease was not due to an increased rate of apoptosis.

Knockdown of SYK in OVCAR-3 cells also resulted in an inability to migrate and was also dependent on kinase activity.

Inhibition of SYK in OVCAR-3 cells increased vimentin expression, indicating a possible role in the epithelial-mesenchymal transition.

Syk is well-documented to be an upstream regulator of a number of pathways depending on cell function. The relevance of this signaling for cancer growth and invasiveness is relatively unexplored.

## References

**Figure 6. Direct and indirect targets of the Syk protein.**

The SYK tyrosine kinase is a critical player in diverse biological functions. Anita Mooker, Jürgen Rüdiger & Victor L. J. Tybulewicz. Nature Reviews Immunology 10, 387-402

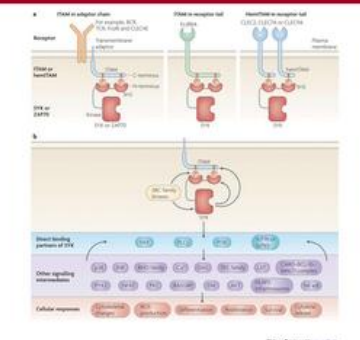


**Table 1: Genomic profiling reveals SYK expression in clinical specimens of ovarian cancer and minimal to absent expression in breast cancers.**

SYK was expressed in ovarian cancers (n = 57) compared to breast cancers (n = 68). The majority of breast cancers (73%) were negative for SYK expression, while 73% of ovarian specimens expressed SYK.

Tissue	Gene Expression			
	Negative	Low	Medium	High
Ovarian	27	22	42	9
Breast	73	23	3	0

**Figure 1: Syk expression in ovarian cancer cell lines can be silenced using SYK-specific siRNA.**

**Legend. Panel A.** Syk was expressed in six of the ten ovarian cancer cell lines. The cell lines were seeded at a concentration to achieve 30% confluency on the day of the experiment and allowed to attach overnight. Cells were collected after a 48 hr incubation at 37 °C, 5% CO<sub>2</sub>, and total cell proteins extracted using 1x RIPA buffer (10 mM Tris-Cl, pH 8.0, 140 mM NaCl, 1% Triton X-100, 0.1% SDS, and 1% deoxycholic acid) with fresh protease inhibitors. **Panel B.** OVCAR-3 cells transfected with the SYK-specific siRNA inhibitor have >90% knockdown of Syk protein. OVCAR-3 cells were seeded at a concentration to achieve 30% confluency on the day of the experiment and siRNA-Lipofectamine RNAiMax complexes were simultaneously transfected to give a final concentration of 15 nM siRNA. Cells were allowed to attach and collected after a 48 hr incubation at 37 °C, 5% CO<sub>2</sub>. Total cell proteins were extracted using 1x RIPA buffer (10 mM Tris-Cl, pH 8.0, 140 mM NaCl, 1% Triton X-100, 0.1% SDS, and 1% deoxycholic acid) with fresh protease inhibitors. Under these conditions, the SYK gene product was silenced >90% relative to OVCAR-3 wild-type cells and scrambled controls. Blots in panel A & B were re-probed with an anti-alpha tubulin antibody to verify equal protein loading among the various conditions.

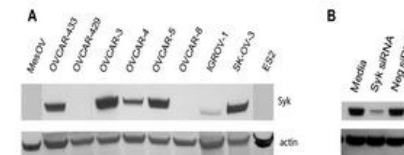


**Figure 2: Knockdown of SYK expression or inhibition of SYK activity decreases cell density.**

**Legend.** Examination of Syk effects on cell density. OVCAR-3 cells plated in 96-well tissue culture plates were grown in media with 10% FBS and reached confluence within 96hrs. When these cells were transfected with the same SYK-specific siRNA (15 nM final concentration), confluence was delayed when compared to cells grown in media. Cells transfected with the scrambled siRNA, Neg (15 nM final concentration), showed minimal effects on the ability of these cells to reach confluence. Inhibition of the kinase activity for Syk with P505 resulted in a similar decrease in confluence, suggesting that kinase activity is required. All cells were incubated at 37 °C, 5% CO<sub>2</sub> (total time 96 hrs). Cell density (Y-axis) was assessed by the sulforhodamine blue (SRB) assay. (n=3)

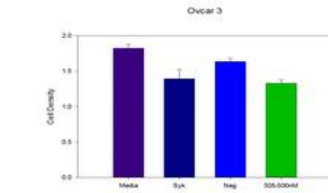


**Figure 3: Inhibition of Syk does not result in an increased rate of apoptosis.**

**Legend.** OVCAR-3 cells transfected with the SYK-specific or non-targeting siRNA (15 nM), or lipofectamine RNAiMax alone for 24 hr. Cells were then exposed to paclitaxel for either 24 hr (Upper panel) or 48 hr (Lower Panel). The cells were then harvested using trypsin without EDTA, and stained with an enhanced green fluorescent protein (EGFP) fused with annexin V and propidium iodide (PI). Flow cytometry was performed and FACS plots were compared to untreated controls. All cells were incubated at 37 °C, 5% CO<sub>2</sub>.

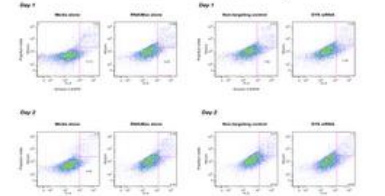


**Figure 4: Inhibition of Syk expression or Syk kinase activity resulted in decreased capability of cells to migrate.**

**Legend.** OVCAR-3 cells were plated in 6-well tissue culture plates with media alone, transfected with the SYK-specific siRNA (15 nM) or Neg-siRNA (scrambled; 15 nM), or with P505 at the time of seeding. Cells were allowed to grow to 80% confluence. The solution in all wells was then replaced with media containing 1% FBS and cells allowed to grow and additional 24hrs. A wound scratch was then performed (indicated by time 0hr). Following a 24 hr incubation, the cells were re-examined and degree of migration noted (indicated by time 24hr). Cells were incubated at 37 °C, 5% CO<sub>2</sub> (total time 120hrs). 10x magnification under confocal microscopy.

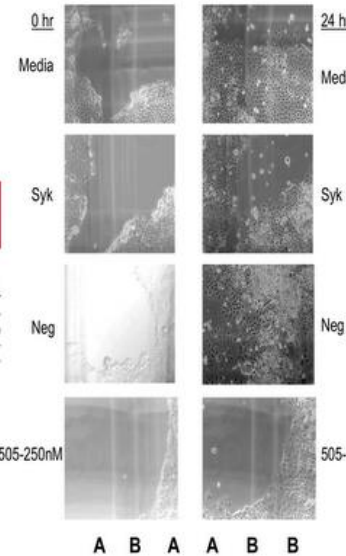


**Figure 5: OVCAR-3 cells transfected with the SYK-specific siRNA result in increased vimentin expression.**

**Legend.** OVCAR-3 cells were seeded in the LAB-TEK II 4-well chamber slide in the presence of media alone or transfected with Syk-siRNA (15 nM). Cells were incubated at 37 °C, 5% CO<sub>2</sub> for 72hrs and then immunostaining was performed with the nuclear stain (DAPI), IgG control antibody (not shown), or vimentin (VIM). **Top Panel.** Ovar 3 cells grown in media alone. DAPI (A) and VIM (B) staining; overlay of DAP and VIM (C). **Lower Panel.** OVCAR-3 cells transfected with Syk-specific siRNA inhibitor (15 nM). DAPI (A) and VIM (B) staining; overlay of DAP and VIM (C).

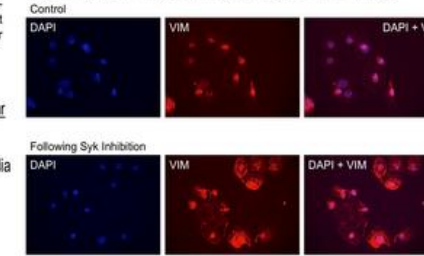
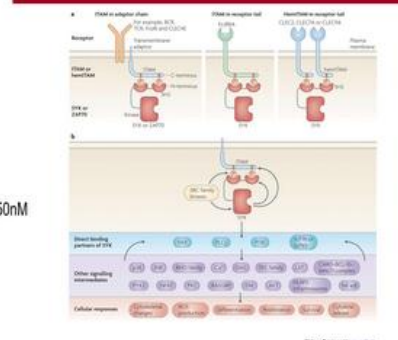


**Figure 6. Direct and indirect targets of the Syk protein.**

The SYK tyrosine kinase is a critical player in diverse biological functions. Anita Mooker, Jürgen Rüdiger & Victor L. J. Tybulewicz. Nature Reviews Immunology 10, 387-402



Too much text

# O<sup>6</sup>-Benzylguanine Inhibits Tamoxifen Resistant Breast Cancer Cell Growth and Resensitizes Breast Cancer Cells to Anti-Estrogen Therapy

Joshua Smith<sup>1</sup>, George C Bobustue<sup>1</sup>, Rafael Madero-Visbal<sup>1</sup>, Jimmie Colon<sup>1</sup>, Beth Isley<sup>1</sup>, Jonathan Ticku<sup>1</sup>, Kalkunte S. Srivenugopal and Santhi Konduri<sup>1</sup>

<sup>1</sup>Cancer Research Institute of M.D Anderson Cancer Center Orlando <sup>2</sup>Texas Tech University Health Sciences Center, Amarillo, TX



SUPPORTED BY THE CHARLES LEWIS INSTITUTE



## Abstract

Endocrine therapies using anti-estrogens are less toxic and very effective for breast cancers, however, tumor resistance to tamoxifen remains a stumbling block for successful therapy. Based on our recent study on the involvement of the DNA repair protein MGMT in pancreatic cancer (Clna Cancer Res. 15, 6608-2009), here, we investigated whether MGMT overexpression mediates tamoxifen resistance. Specifically, we demonstrated altered abundance of MGMT inhibitor O<sup>6</sup>-benzylguanine (BG) at a non-toxic dose in tamoxifen resistant breast cancer cells. Our experiments showed that BG alone or BG in combination with tamoxifen or fulvestrant decreased ER-α expression, whereas tamoxifen alone and fulvestrant also increased and decreased the same respectively. However, all these treatments increased the p21<sup>waf1</sup> mRNA and protein expression significantly. BG inhibited tamoxifen resistant breast cancer growth in a dose-dependent manner and it also resensitized resistant breast cancer cells to anti-estrogen therapy (TAM/ICI). These combinations also enhanced the cytochrome C release and the PARP cleavage, indicative of apoptosis. In breast cancer xenografts, BG alone or a combination of BG with tamoxifen or fulvestrant caused significant tumor growth delay and immunohistochemistry revealed that BG inhibited the expression of MGMT, ER-α, ki-67 and increased p21<sup>waf1</sup> staining. These findings suggest that MGMT inhibition may provide a novel and effective approach for overcoming tamoxifen resistance.

MGMT expression was found to be increased in breast cancer cells relative to normal breast epithelial cells. Also, MGMT levels were significantly higher in tamoxifen resistant breast cancer cells. The ER-α expression using a specific siRNA treatment. Our experiments showed that BG alone or BG in combination with tamoxifen or fulvestrant decreased ER-α expression, whereas tamoxifen alone and fulvestrant also increased and decreased the same respectively. However, all these treatments increased the p21<sup>waf1</sup> mRNA and protein expression significantly. BG inhibited tamoxifen resistant breast cancer growth in a dose-dependent manner and it also resensitized resistant breast cancer cells to anti-estrogen therapy (TAM/ICI). These combinations also enhanced the cytochrome C release and the PARP cleavage, indicative of apoptosis. In breast cancer xenografts, BG alone or a combination of BG with tamoxifen or fulvestrant caused significant tumor growth delay and immunohistochemistry revealed that BG inhibited the expression of MGMT, ER-α, ki-67 and increased p21<sup>waf1</sup> staining. These findings suggest that MGMT inhibition may provide a novel and effective approach for overcoming tamoxifen resistance.

## Introduction

Recent advances in breast cancer research have identified key pathways involved in the repair of DNA damage induced by chemotherapeutic agents. The ability of cancer cells to recognize DNA damage and initiate DNA repair is an important mechanism for therapeutic resistance and has a negative impact on therapeutic efficacy. A number of DNA-damaging alkylating agents attack the nucleophilic O<sup>6</sup> position on guanine, forming mutagenic and highly cytotoxic interstrand DNA crosslinks. The DNA repair enzyme O<sup>6</sup>-methylguanine DNA methyltransferase (MGMT), encoded by the gene MGMT, repairs alkylating agents by preferentially protecting both tumor and normal cells from alkylating agents. MGMT is expressed constitutively in normal cells and tissues. In breast cancer, MGMT gene expression is elevated and levels are up to 4-fold higher than in normal breast epithelial cells. MGMT overexpression has been associated with tamoxifen resistance in breast cancer. Tamoxifen (TAM) is a selective estrogen receptor modulator (SERM) that acts as an anti-estrogen in breast cancer cells. It inhibits MGMT and p53 tumor suppressor proteins when wild-type p53 suppresses MGMT transcription. MGMT function is often inactivated or suppressed in tamoxifen resistant breast cancer cells. The success of some treatments. However, whether or not this is mediated by suppression of MGMT expression has yet to be determined. To date, the cross-talk between MGMT and ER-α (and the link to p53 expression) has not been explored in drug (i.e., tamoxifen) resistant breast tumors. The anti-estrogen tamoxifen is the most commonly used treatment for patients with estrogen receptor positive breast cancer. Although many patients benefit from tamoxifen in the adjuvant and metastatic settings, resistance to this endocrine therapeutic agent is an important clinical problem. The primary goal of present study was to investigate the mechanisms of anti-estrogen drug resistance and to design new therapeutic strategies for overcoming this resistance. The results show that MGMT expression is increased in TAM-resistant breast cancers and inhibition of MGMT by BG significantly improves TAM-sensitivity.

## Results

**Prolonged Treatment of Tamoxifen Increases MGMT Expression:** We developed a tamoxifen resistant MCF-7 cell line by using prolonged treatment of tamoxifen on the parental ER-positive breast cancer cell line, MCF-7. Tamoxifen-resistant MCF-7 cells proliferate at rates similar to the parental MCF-7. Prolonged treatment of tamoxifen onto MCF-7 cells increased MGMT expression compared to parental MCF-7 cells by 2 fold (Fig. 1).

**Knocking Down ERα Enhances MGMT Expression in Tamoxifen Resistant Breast Cancer Cells:** It is not known whether ERα and MGMT transcriptionally regulate each other in tamoxifen resistant breast cancer cells. We therefore investigated whether down regulation of ERα has any effect on endogenous MGMT expression in these cells. As expected, downregulation of ERα using specific siRNA significantly reduced ERα protein levels in these cells. Western blot analysis was performed and the results in the left panel (Fig. 2A) shows that silencing of ERα increases MGMT expression in these cells, and interestingly, the results in the right panel (Fig. 2B) show increased MGMT mRNA levels were increased as assessed by qRT-PCR. These data suggest that ERα-mediated signaling functions to repress MGMT gene expression in breast cancer cells.

**Transcriptional Regulation Between MGMT and p53:** Previously, it was reported that p53 negatively regulates MGMT in breast cancer cells. Therefore, we addressed whether or not silencing the p53 enhances endogenous MGMT transcription. Tamoxifen resistant MCF-7 cells were transfected with either p53 siRNA (p53-KD) (Fig. 2C) or MGMT siRNA (MGMT-KD) (Fig. 2D) along with Non-specific siRNA (NS). MGMT expression was consistently increased in p53 knock down cells, with different experiments showing a ~ 5 fold augmentation (Fig. 2A) and as expected, knocking down MGMT decreased MGMT transcription where as p53 mRNA levels were unaffected in MGMT knockdown cells (Fig. 2D). These results confirm that p53 can regulate MGMT at the transcriptional level.

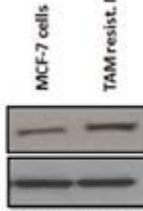


Figure 1. MCF-7 parental and tamoxifen resistant MCF-7 cell cultures were prepared. Proteins were isolated and MGMT expression was detected by western blot analysis. Tamoxifen resistant MCF-7 breast cancer cells significantly increased MGMT expression compared to MCF-7 parental cells.

**O<sup>6</sup>-Benzylguanine Plays a Dual Role in Tamoxifen Resistant MCF-7 Cells:** Contrasting with the experiments above, next, we studied whether or not knocking down MGMT has any effect on ERα transcription. As expected, knocking down MGMT decreased MGMT gene transcription. However, it was interesting to find that ERα gene transcription was also reduced after MGMT silencing (Fig. 2E). These data demonstrate that BG has the ability to attenuate the not only the MGMT, but also the ERα transcription, indicating a possible dual role for MGMT blockers in these breast cancer cells.

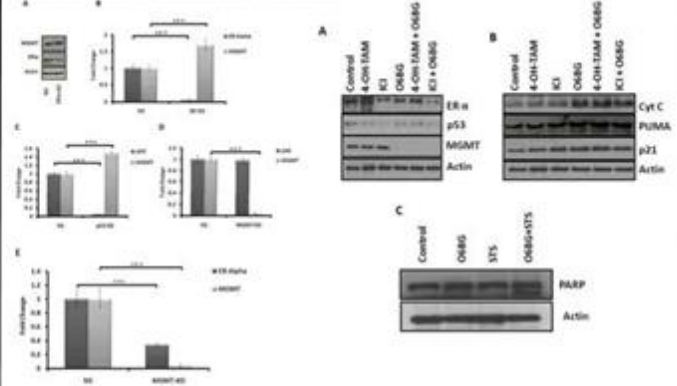


Figure 2. (A) Tamoxifen resistant MCF-7 breast cancer cells were treated in the presence or absence of O<sup>6</sup>-benzylguanine (O<sup>6</sup>BG), tamoxifen (TAM), or ICI (ICI) alone or in combination with O<sup>6</sup>BG or TAM. MGMT mRNA levels were determined by qRT-PCR. (B) ERα and p53 mRNA levels were determined by qRT-PCR. (C) Total RNA was isolated from non-specific siRNA (NS) control and MGMT siRNA (MGMT-KD) knock down tamoxifen resistant MCF-7 breast cancer cells. MGMT and p21 transcription was determined by qRT-PCR. There is an inverse correlation between MGMT and p21 in tamoxifen resistant breast cancer cells. (D) ERα, p53, and ki-67 mRNA levels were determined by qRT-PCR. (E) ERα and p53 mRNA levels were determined by qRT-PCR. There is an inverse correlation between MGMT and p53 in tamoxifen resistant breast cancer cells. (F) ERα, p53, and ki-67 mRNA levels were determined by qRT-PCR. There is an inverse correlation between MGMT and p53 in tamoxifen resistant breast cancer cells.

**O<sup>6</sup>-Benzylguanine Modulates p53 Down-Stream Targeted Protein Expressions:** Encouraged by the results reported, we investigated the effect of combination therapy on endogenous MGMT, p53, and ERα protein expressions. As expected, BG decreased MGMT expression, while combination therapy (4-OH-TAM or ICI) combined with BG significantly decreased both MGMT and ERα expressions. BG alone or in combination with tamoxifen or ICI decreased ER-α expression, whereas tamoxifen alone and ICI also increased and decreased the same respectively (Fig. 3A). p53 expression was slightly altered after ICI treatment. The reduction in p53 expression by ICI alone was reversed when BG was combined (Fig. 3A). We investigated the effect of BG on proteins which are involved in cell cycle regulation, apoptosis in tamoxifen resistant breast cancer cells. All these treatments significantly increased the p21<sup>waf1</sup> protein expression (Fig. 3B). PUMA expression was also increased with these treatments. Hence, PUMA may have translocated to the mitochondria, cytochrome C is released and apoptosis is triggered in these cells in presence of combination therapy. PARP cleavage is seen in BG treated cells in presence of staurosporin as an indicative of apoptosis (Fig. 3C). Therefore, this data suggest that BG promotes cell cycle arrest and can induce apoptosis by modulating p53 function.

**O<sup>6</sup>-Benzylguanine Modulated Transcriptional Targets in Tamoxifen Resistant Breast Cancer Cells:** The effect of combination therapy on endogenous MGMT mRNA levels was also studied. Quantitative real-time PCR (qRT-PCR) revealed that anti-estrogen (TAM/ICI) increased the MGMT expression while the combination therapy decreased it compared to control levels. ERα transcription was decreased compared to controls with all these treatments (Fig. 4A). Surprisingly, p21 and PUMA mRNA was significantly increased in the presence of combination treatments (Fig. 4B). These results clearly demonstrate that BG significantly enhanced p21 transcriptional activity by 4 fold in these cells (Fig. 4D).

**O<sup>6</sup>-Benzylguanine Enhances p53 Transcriptional Activity in Tamoxifen Resistant Breast Cancer Cells:** In order to investigate the effect of BG on p53 function, we performed luciferase reporter assays. Tamoxifen resistant MCF-7 breast cancer cells were transfected with pGL3 promoter construct in presence or absence of BG (large dose of p53). These results clearly demonstrate that BG significantly enhanced p21 transcriptional activity by 4 fold in these cells (Fig. 4D).

Figure 3. Tamoxifen resistant MCF-7 breast cancer cells were treated in presence or absence of BG (10 μM) and fulvestrant (ICI) (100 nM) or tamoxifen (TAM) (100 nM) or combinations. (A) MGMT and ERα (B) p53 transcription (C) PUMA transcription was determined by qRT-PCR. (D) 4-OH-TAM and ICI induced MGMT expression. BG induced PUMA and p21 transcription. (E) Tamoxifen resistant MCF-7 breast cancer cells were transfected with p21 luciferase reporter construct and 48 later treated with BG and 48 later cells were harvested. p21 transcriptional activity was significantly increased by BG in these cells.

**O<sup>6</sup>-Benzylguanine Inhibits Tamoxifen Resistant Breast Cancer Cell Growth and Increase Resistant Breast Cancer Cell Sensitivity to Anti-Estrogen Therapy (TAM/ICI):** Detailed necropsy revealed that all the breast tumors in the breast. The data summarized in Table 1 show the daily BG alone or in combination with tamoxifen or fulvestrant significantly decreased median tumor volume and weight as compared with that seen in tamoxifen/ICI treated and control mice. The combination of BG with tamoxifen or ICI produced the greatest decrease in median tumor volume as compared with control mice (83.99 mm<sup>3</sup>, 9.33 mm<sup>3</sup> (TAM+BG), respectively; p<0.0001, 83.99 mm<sup>3</sup>, 21.60 mm<sup>3</sup> (ICI+BG), respectively; p<0.0001). Tumor weight was also significantly reduced in mice treated with combination therapy as compared with control mice (80.23 mg, 22.39 mg (TAM+BG), respectively; p<0.0001, 83.99 mm<sup>3</sup>, 21.60 mm<sup>3</sup> (ICI+BG), respectively; p<0.0001). Body weight was not affected among all treatment groups as compared with control mice. No visible liver metastases were seen in any of the treatment groups.

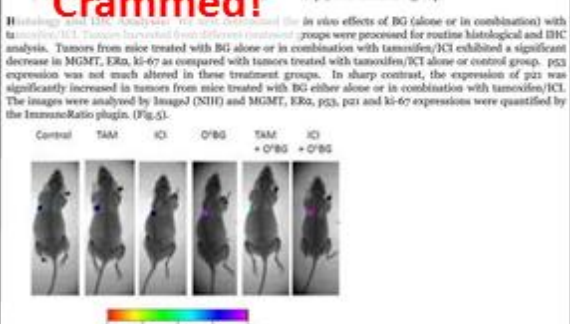


Figure 4. Tamoxifen resistant MCF-7 breast cancer cells were treated in the presence or absence of BG (10 μM) and fulvestrant (ICI) (100 nM) or tamoxifen (TAM) (100 nM) or combinations. (A) MGMT and ERα (B) p53 transcription (C) PUMA transcription was determined by qRT-PCR. (D) 4-OH-TAM and ICI induced MGMT expression. BG induced PUMA and p21 transcription. (E) Tamoxifen resistant MCF-7 breast cancer cells were transfected with p21 luciferase reporter construct and 48 later treated with BG and 48 later cells were harvested. p21 transcriptional activity was significantly increased by BG in these cells.

**Histology and IHC Analysis:** The *in vivo* effects of BG (alone or in combination) with tamoxifen/ICI on tumor growth and sensitivity to anti-estrogen therapy were assessed by routine histological and IHC analysis. Tumors from mice treated with BG alone or in combination with tamoxifen/ICI exhibited a significant decrease in MGMT, ERα, ki-67 as compared with tumors treated with tamoxifen/ICI alone or control group. p53 expression was not much altered in tumors from mice treated with BG either alone or in combination with tamoxifen/ICI. The images were analyzed by ImageJ (NIH) and MGMT, ERα, p53, p21 and ki-67 expressions were quantified by the Immunoprofit plugin. (Fig. 5).



Figure 5. Tumors were harvested from control mice and mice treated with tamoxifen/ICI, BG, or both tamoxifen/ICI and BG. The sections were immunostained for expression of MGMT, ERα, p53 and ki-67. Tumors from mice treated with BG either alone or in combination with tamoxifen or ICI had a significant decrease in the expression of MGMT, ERα and ki-67. p53 expression was not much altered in these treatment groups. In sharp contrast, expression of p21 was significantly increased in all these treatment groups compared to controls. Representative samples (40X are shown).

- ### Conclusions
- In the present study, we observed that prolonged treatment with anti-estrogen causes drug resistance by inducing the DNA repair protein O<sup>6</sup>-methylguanine DNA methyltransferase (MGMT).
  - Decreasing the expression of MGMT by exposing breast cancer cells to BG sensitized these cells to anti-estrogen therapy (tamoxifen and ICI) (80,23%).
  - We also observed that combination therapy of anti-estrogen and MGMT blockers not only overcome the MGMT derived drug (tamoxifen and ICI) resistance but also increased the efficacy of anti-estrogen therapy by decreasing estrogen receptor expression and restoring the functional activity of p53 in tamoxifen-resistant breast cancer cells.
  - Combination therapy inhibited tamoxifen resistant breast tumor growth *in vivo*.

### Acknowledgements

We would like to thank the Florida Department of Health, South Florida Cancer Research Program (SFCR) for the kind funding of this project.

# Tips for Designing Effective Presentations

*A poster with the main title in 1 1/2" sans serif*

Developed by D. Strong, C. Dwyer, W. Kirby, B. Immel, and K. Wink  
with materials donated by Penn State Education Technology Services

Get the audience's attention and communicate your message quickly and succinctly.



Display your design clearly. Plan to capture all the design ideas regarding content, branding, titles, statistics, charts, maps, and how to arrange it.

**A** successful poster presents you and your work clearly and professionally. It communicates the information in a way that can be read and understood. The main title is the most important part of the poster.

## Planning

Keep it simple.  
Display an informative hierarchy.  
Think visually.

## Developing a Layout

The most important thing you should do is plan to keep things aligned and straight.  
Use a 1/2" margin.  
Use a uniform format.  
Try making 40% of the poster your image of the information.  
Leave more room of focus and text.  
If making up information, just make sure to add color.



If you work in the design you can find guides to help you find the right color to use. Above the color wheel is a color wheel to help you find the right color to use.



Planning the layout of the poster is the most important part of the design process.

## Choosing and Using Color

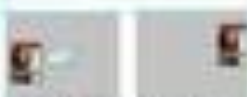
Choose a color scheme.  
Use high-contrast colors. Green and red are good choices for text and graphics.  
The right, unusual color palette.  
Large amounts of text, either in large or medium size settings.

## Selecting Fonts and Using Text

The easiest way to find the right font is to use the font you are using.  
The more you know the better.  
Choose font appearance and consistent sizes.  
The larger font size is the best and the most clear.  
Check out the font for high impact and readability.



"Font" is the letters and symbols in a design. "Type" means "text" or "text" and "text" means "text" or "text".



Be careful that you don't have too much text on your poster. The design should be clear and easy to read.

## Judges Checklist

Remember, the following should be clearly presented and visible from a distance of 10 to 15 feet.

1. Title of the poster
2. Author's name
3. Title, abstract, objectives, and description
4. Funding sources
5. Significant innovative approach or the project's problem (focus on what is new or different from existing work)
6. Methods
7. Significance to the field
8. Significance to society in general
9. Results
10. Conclusions of results and overall goals
11. Acknowledgments for their support

## Using Images

The most important, high-quality images. Appropriate and relevant to design. Use a color image or the appropriate to increase its value.  
Use photos, illustrations, or graphics. Label clearly to help identify and explain.  
Caption clearly and graphically.  
The font size is graphically to be clear and to add additional information.  
Use images to help you understand the data in the poster and help you to find the information you need to read.



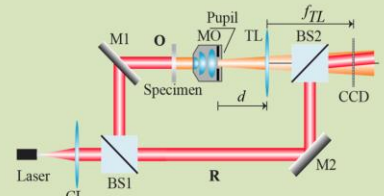
Viewers reading this line demonstrate the poster's success!

A. Doblas, E. Sánchez-Ortiga, M. Martínez-Corral, G. Saavedra and J. Garcia-Sucerquia, "Drawbacks of using non-telecentric geometry in digital holographic microscopy", *Focus Latin America 2014*, Medellín (Colombia), November 2014.

**ABSTRACT**

Digital holographic microscopy (DHM) distinguishes itself from other microscopic techniques to be a powerful method in quantitative phase imaging (QPI). However the main drawback in QPI-DHM is that off-axis DHMs operate in non-telecentric regime. In this contribution, we present the drawbacks on phase measurements and the resolution capability introduced by the arrangement of a non-telecentric imaging system. The problem is that the complex object wavefield imaged in DHM setups presents a quadratic phase factor which turns the DHM into a shift-variant system. Besides the above, the non-telecentric DHM also presents limitations in amplitude contrast imaging. In fact, the presence of the quadratic phase term increases the size of the  $\pm 1$  terms in the Fourier spectrum of the hologram. This broadening makes harder the numerical reconstruction of the image and provides a deteriorated reconstructed image

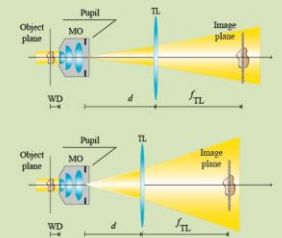
**OFF-AXIS DIGITAL HOLOGRAPHIC MICROSCOPY**



$$H(\mathbf{x}) = |U(\mathbf{x})|^2 + |R(\mathbf{x})|^2 + U(\mathbf{x})R^*(\mathbf{x}) + U^*(\mathbf{x})R(\mathbf{x})$$

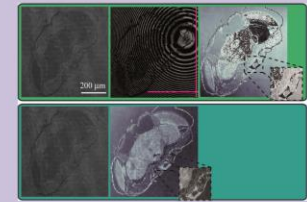
$$U(\mathbf{x}) = \frac{1}{M} \exp(ikL_0) \exp\left(\frac{ik}{2C}|\mathbf{x}|^2\right) \left\{ O\left(\frac{\mathbf{x}}{M}\right) \otimes \tilde{p}\left(\frac{\mathbf{x}}{\lambda f_n}\right) \right\}$$

Lateral magnification  $M = -f_n / f_{MO}$       Radius of curvature  $C = -f_n^2 / (f_n - d)$



☒ In the object distribution it appears a spherical phase factor which perturbs both quantitative phase images and amplitude-contrast images.

**QUANTITATIVE PHASE IMAGING**

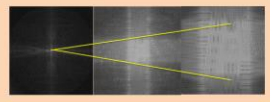


- ☒ Shift-variant property. The accuracy of QPI-DHM can be controlled by the quantity  $C$ .
- ☒ Extra manipulation of the recovered phases from non-telecentric DHMs.
- ☒ After numerical compensation, QPIs are distorted.

**AMPLITUDE-CONTRAST IMAGING**

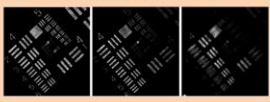
$$\tilde{U}(\mathbf{u}) = \exp(-i\pi\lambda C|\mathbf{u}|^2) \otimes \{ \tilde{O}(M\mathbf{u}) p(\lambda f_n \mathbf{u}) \}$$

The parameter  $C$  controls the size of the  $+1$  term. The  $+1$  term can be understood as a diffraction pattern of the "pure" object spectrum.



Increasing  $1/C$

- ☒ The spatial lateral resolution depends on  $C$  due the spherical phase factor introduce penalties in the spatial filtering.



**REFERENCE**

E. Sánchez-Ortiga et al., "Digital holographic microscopy with pure-optical phase compensation," *J. Opt. Soc. Am. A* **28**, 1410-1417 (2011)  
 A. Doblas et al., "Shift-variant digital holographic microscopy: Inaccuracies in quantitative phase imaging," *Opt. Lett.* **38**, 1352 (2013).  
 E. Sánchez-Ortiga et al., "Off-axis digital holographic microscopy: practical design parameters for operating at diffraction limit," *Appl. Opt.* **53**, 2058 (2014).  
 A. Doblas et al., "Accurate quantitative phase imaging through telecentric digital holographic microscopy," *J. Biomedical Opt.* **19**, 046022 (2014).

# EVALUACIÓN DE LA MICROSCOPIA HOLOGRÁFICA DIGITAL COMO MÉTODO ALTERNATIVO A LA HbA<sub>1c</sub> EN EL DIAGNÓSTICO Y SEGUIMIENTO DE PACIENTES CON DIABETES.

**AUTORES:** A. Doblás<sup>1</sup>, G. Saavedra<sup>1</sup>, M. Martínez-Corral<sup>1</sup>, J. Garcia-Sucerquia<sup>1,2</sup>, E. Roche<sup>3</sup>, F. J. Ampudia-Blasco<sup>4</sup>. **CENTROS:**<sup>1</sup>Universitat de València; <sup>2</sup>Universidad Nacional de Colombia; <sup>3</sup>Universidad Miguel Hernández; <sup>4</sup>H. Clínico Universitario de Valencia.

A. Doblás, G. Saavedra, M. Martínez-Corral, J. Garcia-Sucerquia, E. Roche and F. J. Ampudia-Blasco “Evaluation of digital holographic microscope as an alternative method to the diagnosis and screening of HbA<sub>1c</sub> in diabetic patients,” *XXVI National Meeting on Diabetes (SED), Valencia (Spain), April 2015.*

## RESUMEN

La diabetes es la enfermedad crónica en el mundo de más rápido crecimiento que provocó 5,1 millones de muertes en 2013. La glucosa, a concentraciones elevadas, puede reaccionar no enzimáticamente y de manera irreversible con los grupos amino de las cadenas laterales de aminoácidos proteicos. Las proteínas glucosiladas resultantes muestran cambios en la carga, la estructura y la función, contribuyendo a las complicaciones a largo plazo asociadas con la diabetes. En este contexto, y debido a su larga vida media, la HbA<sub>1c</sub> sirve como un marcador para los niveles medios de glucemia durante largos períodos de tiempo. Dado que la hemoglobina se encuentra dentro de glóbulos rojos circulantes, nuestro objetivo es analizar, cualitativamente y cuantitativamente, los mapas de fase de los eritrocitos en pacientes con DM1 y un grupo normoglucémico mediante microscopía holográfica digital. En particular, también se ha intentado correlacionar estos mapas de fase con la glucemia y HbA<sub>1c</sub>.

## MATERIAL Y MÉTODO

- **Muestra:** Sangre extraída de la vena y un frotis de sangre.
- **Participantes**

	Control (N = 14)		DM1 Pacientes (N=29)	
	Mediana	Rango	Mediana	Rango
Edad (año)	26	22 - 58	40	21 - 55
Altura (cm)	170,5	151 - 190	168	158 - 185
Peso (kg)	72,5	53 - 97	71,6	55,5 - 96,7
Glucosa (mg/dl)	84,5	63 - 120	153	24 - 408
HbA <sub>1c</sub> (%)	5,1	4,5 - 6,0	8,3	6,10 - 10,3

- **Método:** glucómetro (FreeStyle Lite®, Abbott Diabetes Care), cromatografía líquida a alta presión (HPLC) y microscopía Holográfica digital (MHD).



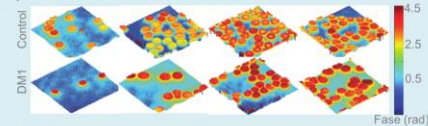
- **Análisis estadístico:** SPSS versión 22.0

## CONCLUSIONES

MHD es una técnica que permite obtener una imagen de fase cuantitativa. En este trabajo, hemos analizado la propiedad óptica de la fase de sujetos afectados por la diabetes a partir de la imagen obtenida con un MHD. A partir de estas medidas, es posible observar diferencias estadísticas en los eritrocitos de los sujetos control y los pacientes DM1. Los valores de fase por encima de 3,40 rad son una indicación de hiperglucemia. Además, a partir de la fuerte correlación entre la HbA<sub>1c</sub> y valores de fase, también podemos suponer que la medición de fase puede proporcionar un índice de glucosa en sangre promedio durante un largo período de tiempo. Este es un trabajo preliminar que requiere más medidas para la correspondiente aprobación clínica del MHD.

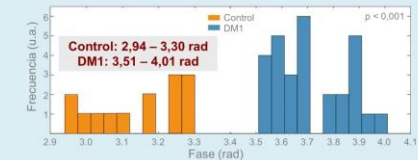
## RESULTADOS-DISCUSSION

### Mapas de fase de los eritrocitos



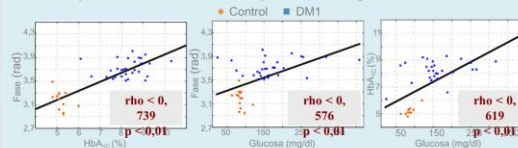
Diferencias de los mapas de fase entre los sujetos sanos y los DM1

### Grupo control vs Pacientes DM1

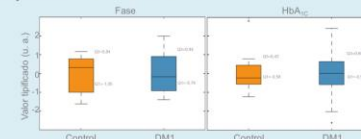


Valor de fase > 3,40 rad indica hiperglucemia

### Comparación con la HbA<sub>1c</sub> y el nivel de glucosa



### Comparación: HPLC vs DHM



**HPLC:** □ Menos insensible a errores y rango amplio para controlar; □ Costoso  
**MHD:** □ Minimamente invasivo, menos tiempo requerido, implementación fácil, detección de cualquier enfermedad donde se cambie las propiedades ópticas de la muestra.

[1] G. Mazurek, T. Freivalds, y A. Jurka. "Properties of erythrocyte light refraction in diabetic patients." *J. Biomed. Opt.* 7(2), 244-247 (2002).  
 [2] F. Okamoto, H. Sone, T. Nonoyama, y S. Homma. "Relative changes in diabetic patients during intensive glycemic control." *Br. J. Ophthalmol.* 84(10), 1097-110 (2000).  
 [3] E. Sánchez-Ortega, A. Doblás, G. Saavedra, M. Martínez-Corral, y J. Garcia-Sucerquia. "Módulo adaptable a un microscopio óptico para obtener imágenes cuantitativas de fase por medio de microscopía holográfica digital (MAMHD)." Patente Española P201331584 (2015).



A. Doblas, E. Boyers, R. L. Blackmon, and A. L. Oldenburg, "Investigation of spectrometer design for reducing roll-off in spectral-domain optical coherence tomography," BiOS 2017, part of Photonics West, San Francisco (USA), January-February 2017.

# Investigating of spectrometer design for reducing roll-off in spectral-domain optical coherence tomography

Ana Doblas<sup>1</sup>, Eric Boyers<sup>1</sup>, Richard L. Blackmon<sup>1</sup>, Amy L. Oldenburg<sup>1,2</sup>

<sup>1</sup>Department of Physics and Astronomy, University of North Carolina - Chapel Hill

<sup>2</sup>Biomedical Research Imaging Center, University of North Carolina - Chapel Hill

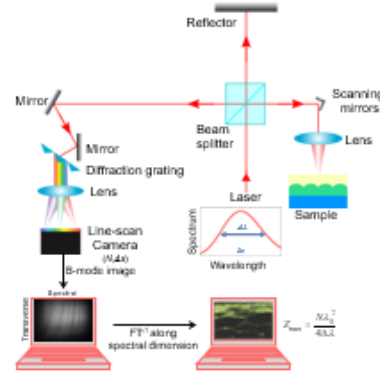
Website: [www.physics.unc.edu/~aold](http://www.physics.unc.edu/~aold); Email: [aold@physics.unc.edu](mailto:aold@physics.unc.edu)



## MOTIVATION

- Spectral-domain optical coherence tomography (SD-OCT) offers depth-resolved images up to a couple of millimeters into a sample with micrometer scale resolution<sup>1,2</sup>.
- SD-OCT typically uses near infrared light sources at low power (~10 mW) making it suitable for biological and biomedical applications.
- Signal roll-off decreases the signal intensity for deeper imaging depth<sup>3</sup>, reducing the image signal to the noise floor and limiting the effective maximum imaging depth.

## SD-OCT Background



In SD-OCT, the light beam proceeding from a laser is split, reflected and re-combined by the beam splitter. The interference between the reference and sample arms is then spatially dispersed by a spectrometer composed of a diffraction grating, a lens and a line scan camera. The B-mode image is obtained after recording the stack of different A-lines and processing them.

### Analysis of one A-line

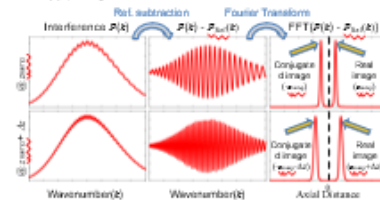
$$P(k) = P_{ref}(k) + P_{sam}(k) + 2\sqrt{P_{ref}(k)P_{sam}(k)}\cos[2\pi k(z_{ref} - z_{sam})]$$

$k = 2\pi / \lambda$ : Wavenumber

$z_{ref}, z_{sam}$ : distance of reflector/sample

$P_{ref}(k)$ : Reference-arm Power

$P_{sam}(k)$ : Sample-arm Power



## SPECTROMETER ROLL-OFF

- Spectrometer acts a low-pass filter on the interference pattern  $P(k)$ , attenuating the frequencies corresponding to larger imaging depths.
- Assuming the spectrum is Gaussian, the light is linearly dispersed on the sensor as a function of wavenumber, and the focal spot size for each wavelength is constant, the intensity rolls off according to<sup>3</sup>

$$I(z) \propto \frac{1}{z} \exp\left(-\frac{\pi}{\ln 2} \frac{\Delta\lambda^2 z^2}{N \lambda_c^2 (\Delta\lambda)^2}\right) \sin\left(\frac{2\pi}{N} \frac{\Delta\lambda}{\lambda_c} z\right)$$

$\Delta\lambda$  = pixel width  
 $N$  = total number of pixel  
 $\lambda_c$  = center wavelength  
 $\Delta\lambda$  = wavelength bandwidth  
 $D$  = beam diameter on spectrometer lens  
 $f_{spec}$  = focal length of spectrometer lens

$$a = \frac{4\lambda_c^2 f_{spec}}{D^2}$$

$a$ : focal spot size

$$R = \frac{2\pi}{N} \frac{\Delta\lambda}{\lambda_c}$$

$R$ : reciprocal linear dispersion

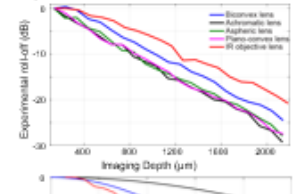
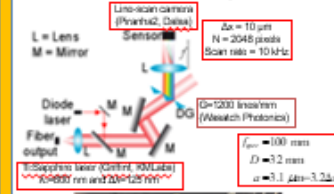
The smaller the value of the spot size ( $a$ ), compared with the pixel size, the less signal roll-off of the spectrometer and the higher maximum imaging depth.

Reducing roll-off in OCT signal by designing a spectrometer with the smallest spot size. The spot size depends on the aberrations of the system. The primary aberrations<sup>4</sup> are the spherical aberration, chromatic aberration, coma, astigmatism and field of curvature.

## EXPERIMENTAL RESULTS

Experimentally measuring the effect of lens type on the signal roll-off in SD-OCT

- Building a spectrometer.
- Use a mirror as a sample and placing at the object focal plane of the imaging lens in the SD-OCT system.
- To measure the roll-off versus imaging depth, translate axially the position of the reference mirror over the imaging depth and record each interference pattern.
- Repeat this measurement for five different spectrometer lenses of the same focal length: an achromatic lens, a plano-convex lens, a biconvex lens, an aspheric lens and an infrared objective.



## CONCLUSIONS

- The spectrometer performance depends on the spot size at the camera plane, the total number of pixels of the camera and the spectral resolution of the spectrometer.
- Using the same camera, the best performance of the spectrometer in term of the signal roll off is achieved by reducing the spot size.
- The spot size depends on the aberrations of the spectrometer's lens.
- Our preliminary experimental results show that the IR objective lens, which has an approximate effective spot size of 14 μm, produces the least signal roll-off in SD-OCT (signal decay of 19 dB in 2 mm). On the contrary, the achromatic and the plano-convex lenses are the worst one (signal loss of 27 dB in 2 mm).

## REFERENCES

[1] J. A. Izatt et al., *Optical coherence tomography: technology and applications*, Chapter 2 (Springer, 2008).  
 [2] W. Chiriac et al., *ASAP*, 28(2), 071412 (2014).  
 [3] Z. Hu et al., *AO* 46(25), 8499-8505 (2007).  
 [4] M. Born et al., *Principle of Optics*, Chapter 5 (Cambridge University Press, 1999).

### Acknowledgments:

This work was supported in part by the Department of Defense, Air Force Office of Scientific Research (Grant #FA9550-14-1-0208)

N. Patwary, A. Doblas, G. Saavedra, and C. Preza, "Implementation of PSF engineering using a fabricated SQUBIC phase mask to reduce the effect of spherical aberration in 3D wide field fluorescence imaging," *Quantitative BioImaging Conference '17*, College Station (Texas, US), January 2017.

## Abstract

Wavefront encoded (WFE) 3D fluorescent imaging is studied with a fabricated squared cubic (SQUBIC) phase mask to reduce the effect of depth-induced aberration. Experimental results demonstrate that the WFE system can produce results predicted by simulations, and intermediate WFE images show 3% variability over a 65  $\mu\text{m}$  imaging depth.

## Summary

### Objective:

To reduce the depth sensitivity of the imaging system by reducing the effect of aberration.

### Benefit:

Making the Image reconstruction process computationally efficient, and at the same time reducing the restoration artifact.

### Application:

Computationally efficient 3D imaging of thick biological cells without damaging them.

## Wavefront Encoding (WFE)

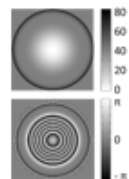
### Modified Imaging System Model

$$h_{i,j}(x, y) = \left| \delta^{-1} \left\{ H(f_x, f_y) e^{i2\pi(xf_x + yf_y)} e^{-i\pi(\lambda z)(f_x^2 + f_y^2)} e^{-i\pi(\lambda z)(f_x^2 + f_y^2)} \right\} \right|^2$$

### SQUBIC Phase mask (PM) used in the imaging path [4]

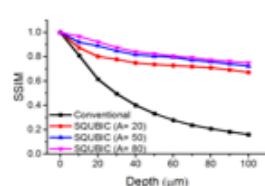
$$p(r, \theta) = \begin{cases} 2\pi r \left[ \frac{\sqrt{1 + f_0^2 \sin^2(\theta)} - 1}{1 - \cos(\theta)} + \frac{1}{2} \right] & ; 0 \leq \sqrt{f_0^2 + 1} \leq 1 \\ 0 & \text{otherwise} \end{cases}$$

Path difference introduced by the Phase Function (used in the fabricated PM)

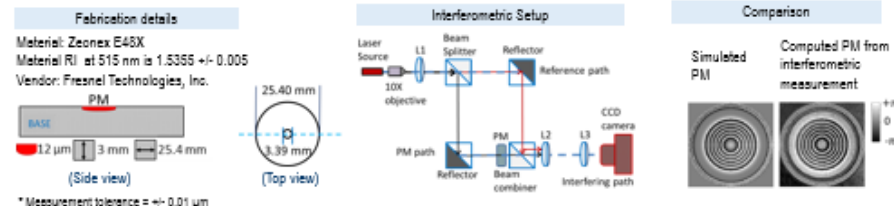


Phase difference produced by the path difference used in spatial light modulator (SLM) based WFE implementation [4].

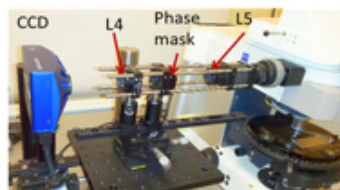
PSF sensitivity comparison between conventional wide field and proposed WFE wide field microscope with respect to depth [5] [quantified by structural similarity index measure (SSIM)].



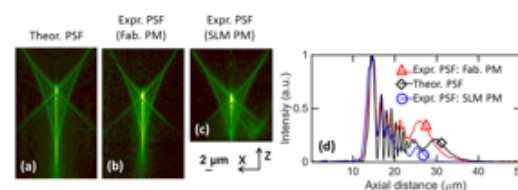
## SQUBIC phase mask (PM) fabrication and performance evaluation



## Experimental Setup



## Wavefront Encoded Imaging System Response



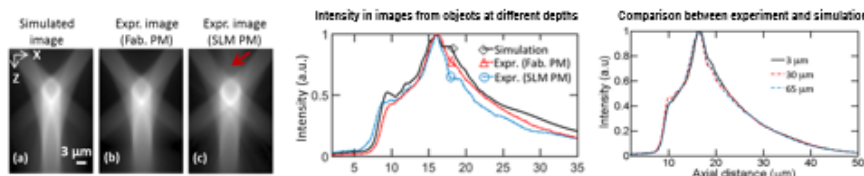
## Experimental Intermediate Image Analysis

### Imaging System:

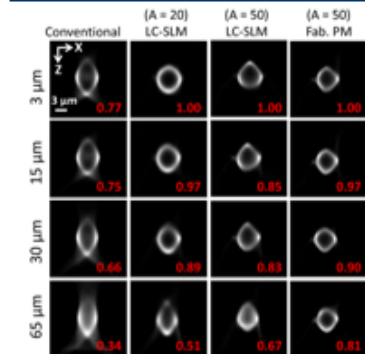
Zeiss Axiocor Z1,  
63X/1.4 NA oil immersion objective lens.  
Specimen Embedding: ProLong Diamond.

### Sample:

- 6  $\mu\text{m}$  in diameter spherical shell.
- Shell thickness is 1  $\mu\text{m}$ .
- Sample depths: 3  $\mu\text{m}$ , 27  $\mu\text{m}$ , and 60  $\mu\text{m}$ .

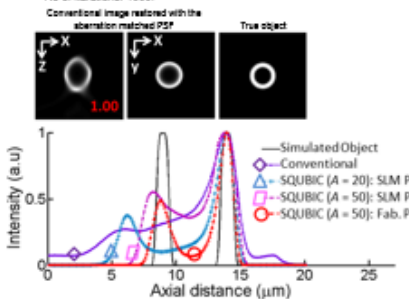


## Experimental Image Reconstruction



### Restoration Method:

- Iterative *space-invariant* regularized expectation-maximization algorithm.
- Restoring PSF: ideal unaberrated PSF.
- No of iterations: 1000.



## Conclusion

- The fabricated PM can implement the desired phase function used in the WFE implementation accurately.
- Intensity distribution of the experimental forward image has a structure similarity index of 0.99 when compared with that of the simulated image, which shows the high implementation accuracy of the WFE system.
- Over the 65  $\mu\text{m}$  depth, intermediate images of the SQUBIC WFE system show a variability of only 3%.
- Images from different depths can be restored with reduced artifact using space-invariant algorithms (which use a single PSF) in the case of SQUBIC WFE system whereas the conventional system requires computationally intensive depth-variant reconstruction algorithms (which use multiple PSFs at different depths [1,2,3]).
- Experimental evaluation of the implemented WFE-COSM system through restoration shows several advantages. The performance of the WFE-COSM system based on the SQUBIC (A = 50) fabricated PM is increased by up to 14% over the SLM-based implementation for the same A.

## Reference

- [1] N. Patwary, H. Shabani, A. Doblas, G. Saavedra, and C. Preza, provisionally accepted in *Applied Optics*, Feature Issue on Modern Imaging.
- [2] N. Patwary, S. V. King, G. Saavedra et al., *Optics Express*, 24(12), 12905-12921 (2016).
- [3] S. V. King, A. Doblas, N. Patwary et al., *Applied Optics*, 54(29), 8587-8595 (2015).
- [4] G. Saavedra, I. Escobar, R. Martínez-Cuenca et al., *Optics Express*, 17(16), 13810-13818 (2009).
- [5] Z. Wang, A. C. Bovik, H. R. Sheikh et al., *IEEE Transactions on Image Processing*, 13(4), 600-612 (2004).

## Acknowledgement

1. National Science Foundation (IDBR award DBI-1353904, PI: C. Preza).
2. "Herff Graduate Fellowship" of the Herff College of Engineering of the University of Memphis, TN, USA.
3. Department of EECE, University of Memphis, TN, USA.
4. The authors are thankful to: S. V. King for help with the experimental setup and for acquiring the SLM-based WFE PSF

# NOVEL STRUCTURED ILLUMINATION IMPROVES 3-D RESOLUTION IN FLUORESCENCE MICROSCOPY

Hasti Shabani<sup>1</sup>, Ana Doblaz<sup>1</sup>, Genaro Saavedra<sup>2</sup>, and Chrysanthe Preza<sup>1</sup>

<sup>1</sup>Computational Imaging Research Laboratory, Department of Electrical and Computer Engineering, The University of Memphis, Memphis, TN 38152

<sup>2</sup>3D Imaging and Display Laboratory, Department of Optics, University of Valencia, Burjassot, Spain.

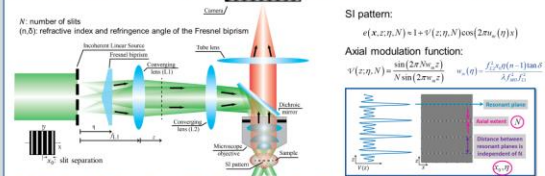
cpreza@memphis.edu

## ABSTRACT

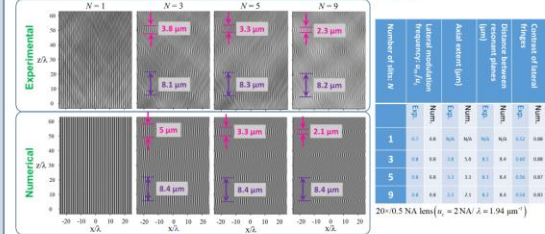
We present the performance of a novel tunable three-dimensional (3D) structured illumination microscope (SIM) system and its ability to provide simultaneously super-resolution (SR) and optical-sectioning (OS) capabilities. The main hallmark of this system is that the final SIM image is restored using 40% less data compared with standard 3D-SIM systems [2]. The performance of the system has been validated experimentally with images from test samples, which were also imaged with a commercial SIM based on incoherent-grid projection [3] for comparison. Restored images from data acquired from an axially-thin fluorescent layer show 1.6x improvement in OS capability compared to the commercial instrument while results from a fluorescent USAF target show a 1.8x improvement in lateral SR capability, which is comparable with the performance of a standard 3D-SIM system [4]. Finally, simultaneous OS and SR capabilities of our 3D-SIM system are verified by imaging a tilted fluorescent USAF test.

## TUNABLE-FREQUENCY 3D-SIM USING A BIPRISM

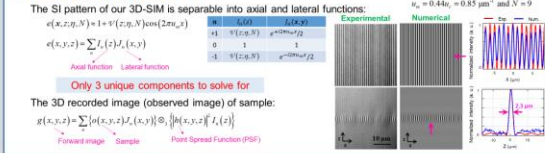
Optical configuration of 3D-SIM system based on Fresnel biprism and multiple slits [1,4]



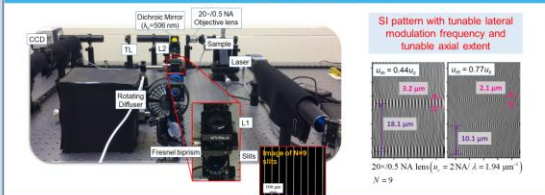
Structured illumination pattern for a different number of slits (N) [1,4]



Forward imaging model [1,7]

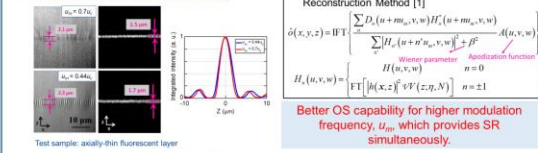


## EXPERIMENTAL SETUP

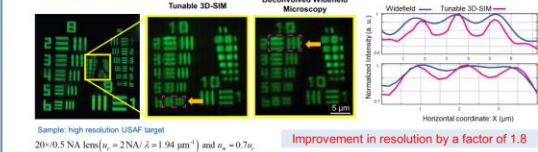


## SYSTEM PERFORMANCE EVALUATION

Optical sectioning (OS) capability



Super-resolution (SR) performance



## COMPARISON WITH COMMERCIAL ApoTome-SIM

Image of a fluorescent layer

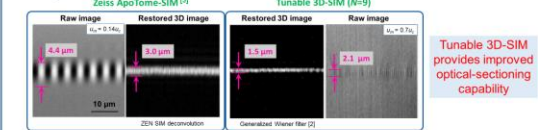
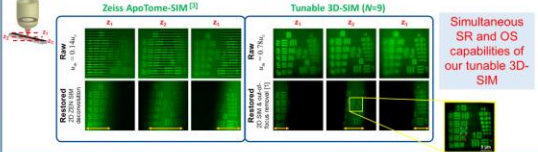


Image of a fluorescent tilted USAF target



## CONCLUSIONS

- 3D illumination pattern with periodic axial extent and tunable lateral modulation frequency (decoupled axial and lateral modulation frequencies).
- System performance validation through comparison of proof-of-concept data with theoretical predictions.
- Improvement in the lateral resolution by a factor of 1.8 while achieving optical sectioning capability.
- Results show potential for improved optical sectioning and super-resolution capabilities achieved with the tunable 3D-SIM system compared to ApoTome SIM.

## REFERENCES

- [1] A. Doblaz et al., *Opt. Express* 26, 30476-30491 (2018).
- [2] M. G. L. Gustafsson et al., *Biophys. J.* 94, 4957 (2008).
- [3] M. A. A. Neil et al., *Opt. Lett.* 22, 1905 (1997).
- [4] C. Karras et al., *bioRxiv* 402115, 1-13 (2018).
- [5] A. Doblaz et al., *JOSA A* 30, 140-148 (2013).
- [6] H. Shabani et al., *Proc. SPIE* 10499, 1049903 (2018).
- [7] H. Shabani et al., *Proc. SPIE* 10070, 1007013 (2017).

## ACKNOWLEDGEMENT

This work is supported by the National Science Foundation (DBI award 1353904, PI: CP) and the University of Memphis (UoM). HS is supported by a Herff graduate fellowship from the Herff College of Engineering, the UoM.

H. Shabani, A. Doblaz, G. Saavedra and C. Preza, "Novel structured illumination improves 3-D resolution in fluorescence microscopy" *Image Science Gordon Research Conference*, Easton (USA), June 2018.

R. Castaneda, C. Trujillo, and A. Doblas, "An Open-Source Python library for Digital Holographic Microscopy Imaging," Poster in *Optica Imaging and Applied Optics Congress, July 2022.*

# An Open-Source Python library for Digital Holographic Microscopy Imaging

Raul Castaneda<sup>1</sup>, Carlos Trujillo<sup>2\*</sup>, and Ana Doblas<sup>1,\*\*\*</sup>

<sup>1</sup>Optical Imaging Research Lab, Department of Electrical and Computer Engineering, The University of Memphis, Memphis, TN 38152, USA

<sup>2</sup>Applied Optics Group, School of Applied Sciences and Engineering, Universidad EAFIT, Medellín, Colombia

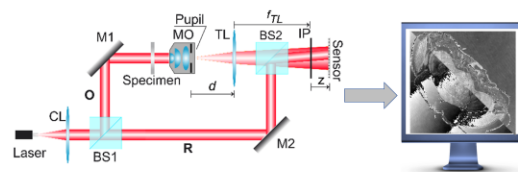
Author e-mail address: catrujilla@eafit.edu.co and adoblas@memphis.edu

## ABSTRACT

Digital holographic microscopes (DHMs) have been widely applied in material and biological applications. The performance of DHM technologies relies heavily on computational reconstruction processing to provide trustworthy sample information. The required reconstruction algorithms are uniquely dependent on the optical configuration of the DHM system; an incorrect selection of the reconstruction algorithms leads to distorted and inaccurate amplitude and phase measurements. In this work, we present an open-source Python library, named pyDHM, containing the needed computational processing approaches to reconstruct DHM images for a wide variety of experimental DHM implementations.

## RECONSTRUCTION ALGORITHMS FOR DIFFERENT OPTICAL DHM CONFIGURATIONS

The selection of the proper computational reconstruction algorithm for a DHM configuration is a critical task to avoid incorrect sample measurements.



### Selection of the reconstruction algorithm

Operation of the DHM system based on the interference angle

- In-line and slightly off-axis DHM systems require phase-shifting algorithms
- Off-axis DHM systems require the spatial filtering of the object spectrum
- Telecentric ( $d = f_{TL}$ ) vs Non-Telecentric DHM systems ( $d \neq f_{TL}$ )
  - The raw phase image is distorted by a spherical phase factor in non-telecentric DHM systems, requiring computational approaches to compensate such distortion.
- In-focus vs out-of-focus holograms
  - Numerical propagators of complex wavefields are required in DHM if the digital holograms are out-of-focus ( $z \neq 0$ ).

## pyDHM LIBRARY STRUCTURE AND EXAMPLES

### Utility Package

- Contains useful functions, such as calculating the hologram spectrum and displaying the amplitude and phase images.
- Functions:
  - imageRead
  - imageShow
  - Amplitude
  - Intensity
  - Phase
  - FT/IFT

### Phase-Shifting Package

- Contains algorithms to reconstruct phase images from inline and slightly off-axis DHMs.
- Functions:
  - PS5 (in-line)
  - PS4 (in-line)
  - PS3 (in-line)
  - SOSR (slightly off-axis)
  - BPS3 (slightly off-axis)
  - BPS2 (slightly off-axis)

### Fully-compensated Phase Reconstruction Package

- Contains algorithms to reconstruct compensated phase images from off-axis DHMs operating at telecentric and non-telecentric regimes.
- Functions:
  - FRS (tele)
  - ERS (tele)
  - CFS (tele)
  - CNT (no tele)

### Numerical Propagation Package

- Contains numerical propagation algorithms to compute the scalar complex amplitude distribution at different propagation distances.
- Functions:
  - Angular Spectrum
  - Fresnel
  - Fresnel-Bluestein

#### Example 1: Reconstructed Phase Image using a blind phase-shifting approach (BPS2) and a slightly off-axis DHM

```

1 # Import libraries
2 import utilies_inl as ui
3 import utilies_display as di
4 import phaseShiftingPhaseShifting as ps
5 # Load the hologram
6 ip = ui.imageRead('holo1.jpg')
7 ip1 = ui.imageRead('holo2.jpg')
8 ip2 = ui.imageRead('holo3.jpg')
9 # Phase shifting via BPS2 or BPS2
10 output = ps.BPS2(ip1, ip2, wavelength, dx, dy)
11 # Display phase reconstruction
12 ip1 = di.phaseReconstr(output)
13 ui.imageShow('Phase Reconstruction')
                    
```

Parameters: wavelength = 0.532 μm, dx = dy = 2.9 μm

#### Example 2: Fully-compensated Reconstructed Phase Image using an off-axis, telecentric-based in-focus hologram (ERS)

```

1 # Import libraries
2 import utilies_inl as ui
3 import utilies_display as di
4 import phaseCompensationPhaseCompensators as pc
5 # Load the hologram
6 hologram = ui.imageRead('hologram.jpg')
7 ui.imageShow('hologram', 'Hologram')
8 # Numerical compensation via ERS approach
9 output = pc.ERS(hologram, wavelength, dx, dy, s, step)
10 # Display intensity and phase reconstruction
11 intensity = di.intensity(output, False)
12 ui.imageShow('intensity', 'Intensity reconstruction')
13 phase = di.phase(output)
14 ui.imageShow('phase', 'Phase reconstruction')
                    
```

Parameters: wavelength = 0.532 μm, dx = dy = 2.4 μm, s = 5, step = 0.2

#### Example 3: Reconstructed Phase Image of an off-axis out-of-focus telecentric-based hologram using the angular spectrum approach

```

1 # Import libraries
2 import utilies_inl as ui
3 import utilies_display as di
4 import phaseCompensationPhaseCompensators as pc
5 # Load the hologram
6 hologram = ui.imageRead('hologram.jpg')
7 ui.imageShow('hologram', 'Hologram')
8 # FT of the hologram
9 ft_holo = di.ft(output)
10 ft_holo = di.intensity(ft_holo, True)
11 ui.imageShow('ft_holo', 'FT hologram')
12 # Circular spatial filter (CSF)
13 filter = di.ft(field, radius, centX, centY)
14 # Numerical compensation angular spectrum
15 output = pr.angularSpectrum(filter, z, wavelength, dx, dy)
16 # Display the intensity reconstruction
17 intensity = di.intensity(output, False)
18 ui.imageShow('intensity', 'Intensity reconstruction')
                    
```

Parameters: wavelength = 0.532 μm, dx = dy = 2.4 μm

## CONCLUSIONS

The pyDHM library, <https://github.com/catruijilla/pyDHM>, is a user-friendly Python library that provides a broad range of reconstruction algorithms for different optical DHM configurations.






## ACKNOWLEDGEMENT

This work was partially funded by the Vicerrectoría de Ciencia, Tecnología e Innovación from Universidad EAFIT, and National Science Foundation (NSF) grant number 2042563.

Driven by doing. THE UNIVERSITY OF MEMPHIS. UNIVERSIDAD EAFIT. Logo

# Objective of the session

At the end of the session, students will be able to

1. Learn the top points for preparing a good poster 
2. Identify best software for drafting a poster 
3. Understand general layout of a poster 
4. Recognize good/bad posters in terms of colors, information and figures  

# Your turn

Find a research poster that you have prepared in the past.

Make a list of improvements based on this lecture. How will you improve it?

